Turn Structures in CGRP C-Terminal Analogues Promote Stable Arrangements of Key Residue Side Chains

Katharine A. Carpenter,*,‡ Ralf Schmidt,‡ Bengt von Mentzer,§ Ulla Haglund,§ Edward Roberts,‡,|| and Chris Walpole‡

Department of Chemistry, AstraZeneca R&D Montreal, 7171 Frédérick-Banting, Saint-Laurent, Québec, Canada H4S 1Z9, and Department of Cell Biology and Biochemistry, AstraZeneca R&D Mölndal, Mölndal, Sweden

Received February 9, 2001; Revised Manuscript Received May 10, 2001

ABSTRACT: The 37-amino acid calcitonin gene-related peptide (CGRP) is a potent endogenous vasodilator thought to be implicated in the genesis of migraine attack. CGRP antagonists may thus have therapeutic value for the treatment of migraine. The CGRP C-terminally derived peptide [D^{31},P^{34},F^{35}]CGRP(27−37)-NH_2 was recently identified as a high-affinity $hCGRP_1$ receptor selective antagonist. Reasonable $CGRP_1$ affinity has also been demonstrated for several related analogues, including [D^{31},A^{34},F^{35}]CGRP(27−37)-NH_2. In the study presented here, conformational and structural features in CGRP(27−37)-NH_2 analogues that are important for $hCGRP_1$ receptor binding were explored. Structure−activity studies carried out on [D^{31},P^{34},F^{35}]CGRP(27−37)-NH_2 resulted in [D^{31},P^{34},F^{35}]CGRP(30−37)-NH_2, the shortest reported CGRP C-terminal peptide analogue exhibiting reasonable $hCGRP_1$ receptor affinity (K_i = 29.6 nM). Further removal of T^{30} from the peptide's N-terminus greatly reduced receptor affinity from the nanomolar to micromolar range. Additional residues deemed critical for $hCGRP_1$ receptor binding were identified from an alanine scan of [A^{34},F^{35}]CGRP(28−37)-NH_2 and included V^{32} and F^{37}. Replacement of the C-terminal amide in this same peptide with a carboxyl, furthermore, resulted in a greater than 50-fold reduction in $hCGRP_1$ affinity, thus suggesting a direct role for the amide moiety in receptor binding. The conformational properties of two classes of CGRP(27−37)-NH_2 peptides, [D^{31},X^{34},F^{35}]CGRP(27−37)-NH_2 (X is A or P), were examined by NMR spectroscopy and molecular modeling. A β-turn centered on P^{29} was a notable feature consistently observed among active peptides in both series. This turn led to exposure of the critical T^{30} residue to the surrounding environment. Peptides in the A^{34} series were additionally characterized by a stable C-terminal helical turn that resulted in the three important residues (T^{30}, V^{32}, and F^{37}) adopting consistent interspatial positions with respect to one another. Peptides in the P^{34} series were comparatively more flexible at the C-terminus, although a large proportion of the [D^{31},P^{34},F^{35}]CGRP(27−37)-NH_2 calculated conformers contained a γ-turn centered on P^{34}. These results collectively suggest that turn structures at both the C-terminus and N-terminus of CGRP(27−37)-NH_2 analogues may help to appropriately orient critical residues (T^{30}, V^{32}, and F^{37}) for $hCGRP_1$ receptor binding.

Calcitonin gene-related peptide (CGRP)[1] is a 37-amino acid neuropeptide characterized by an N-terminal C^2−C^7 disulfide-bonded loop and an amidated C-terminus (*1*). Its two forms (α and β) originate from separate genes and are distinguished by residues at positions 3, 22, and 25 (Figure 1). The neuropeptide is expressed predominantly in neuronal tissues located throughout the periphery and central nervous systems (*2*, *3*). Many biological effects are mediated by CGRP as a consequence of its wide distribution. Most notable is CGRP's stimulatory actions in peripheral blood vessel dilation. CGRP-induced cranial vessel dilation in particular is thought to be linked with the onset of migraine headache (*4*, *5*). Further support for this hypothesis stems from the observed increases in CGRP levels following migraine attack (*6*, *7*). Hence, inhibitors of CGRP-mediated vasodilation are clearly of therapeutic value for the treatment of migraine symptoms.

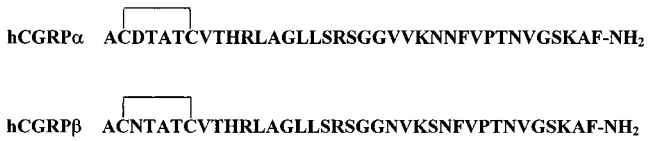

FIGURE 1: Primary structure of human CGRP and its α- and β-isoforms. The single disulfide bridge in each peptide is indicated with a solid line.

* To whom correspondence should be addressed: AstraZeneca R&D Montréal, 7171 Frédérick-Banting, Saint-Laurent, Québec, Canada H4S 1Z9. Telephone: (514) 832-3200. Fax: (514) 832-3232. E-mail: katharine.carpenter@astrazeneca.com.

‡ Department of Chemistry, AstraZeneca R & D Montreal.

§ Department of Cell Biology and Biochemistry, AstraZeneca R & D Mölndal.

|| Current address: F. Hoffman LaRoche Ltd. Pharmaceuticals Division PRPV, Building 015/203, CH-4070 Basel, Switzerland.

[1] Abbreviations: CGRP, calcitonin gene-related peptide; NMR, nuclear magnetic resonance; CD, circular dichroism; NOESY, nuclear Overhauser enhancement spectroscopy; TOCSY, total correlation spectroscopy; TSP, (3,3,3-trimethylsilyl)propionate; SDS, sodium dodecyl sulfate; NOE, nuclear Overhauser enhancement; HATU, *O*-(7-azabenzotriazol-1-yl)-1,1,3,3-tetramethyluronium hexafluorophosphate; TFE, trifluoroethanol; SK-N-MC, neuroepithelioma cell line of human origin.

10.1021/bi0102860 CCC: $20.00
Published on Web 06/21/2001

Table 1: $hCGRP_1$ Receptor Affinities for CGRP(27−37)-NH_2 Analogues

no.	peptide	sequence	binding ([^{125}I]CGRP) SK-N-MC mem K_i (nM)
1	human αCGRP**(8−37)**	VTHRLAGLLSRSGGVKNNFVPTNVGSKAF-NH_2	3.5 ± 1.3
2	[A^{34},F^{35}]CGRP(28−37)-OH	VPTNVGAFAF-OH	>30000
3	[D^{31},A^{34},F^{35}]CGRP(27−37)-NH_2	FVPTDVGAFAF-NH_2	36.5 ± 29.0 (lit. 159)[a]
4	[A^{34},F^{35}]CGRP(27−37)-NH_2	FVPTNVGAFAF-NH_2	88 ± 23.1
5	[A^{34},F^{35}]CGRP(28−37)-NH_2	VPTNVGAFAF-NH_2	495 ± 120
6	[A^{34},F^{35}]CGRP(30−37)-NH_2	TNVGAFAF-NH_2	243 ± 42
7	[A^{34},F^{35}]CGRP(31−37)-NH_2	NVGAFAF-NH_2	19300 ± 7600
8	[D^{31},P^{34},F^{35}]CGRP(27−37)-NH_2	FVPTDVGPFAF-NH_2	6.56 ± 2.01 (lit. 29)[a]
9	[D^{31},P^{34},F^{35}]CGRP(30−37)-NH_2	TDVGPFAF-NH_2	29.6 ± 6.1
10	[D^{31},P^{34},F^{35}]CGRP(31−37)-NH2	DVGPFAF-NH_2	7200 ± 4200

[a] In parentheses, IC_{50} values for peptides as determined by Rist et al. (*22*).

The actions of CGRP are mediated through its interaction with G-protein-coupled receptors. So far, only one CGRP receptor has been cloned, termed the $CGRP_1$ receptor (*8*), whereas a second receptor subtype ($CGRP_2$) has been identified mainly on the basis of pharmacological evidence (*9*, *10*). Structure−activity studies carried out on CGRP analogues have identified regions of the molecule that are important for eliciting either an agonist or antagonist response. N-Terminal fragments of CGRP interact with their receptors in an agonist fashion, with CGRP(1−15) being the shortest active fragment (*11*, *12*). Conversely, C-terminal fragments of CGRP behave as competitive antagonists (*13*, *14*). The analogue CGRP(8−37)-NH_2 is the most potent CGRP antagonist among the reported natural sequences, although further truncation at the N-terminus, up to and including F^{27}, has resulted in reasonably potent antagonists. Substitution of the N-terminal phenylalanine in CGRP(27−37)-NH_2 with a tyrosine did not reduce antagonist activity (*14*, *15*).

Conformational studies have been carried out on CGRP and several of its analogues. The conformational ensemble of CGRP in aqueous solution was determined to be 20% helical on the basis of the results from circular dichroism measurements (*16*). The amount of helicity was increased to 60% in a TFE/water solution (*16*, *17*). Results from NMR studies of CGRP have shown that the helix lies within the V^8−R^{18} region (*18*). A substantial loss of CGRP's helical structure was noted following removal of its N-terminal loop structure (*19*). This has led to a hypothesis suggesting a role for the disulfide-bonded loop structure in promoting agonist activity via stabilization of a helical conformation. However, the helix is more likely implicated in receptor binding than receptor activation since an increase in the antagonist potency of CGRP(8−37)-NH_2 occurred upon replacement of specific residues in the proposed helical region with the helix-promoting residue alanine (*20*). Conversely, in most of the reported structures for CGRP and its analogues, the C-terminus is described as being conformationally disordered, although evidence of a turn structure centered on G^{33} was obtained from modeling investigations (*17*, *21*).

Rist et al. (*22*) recently performed a complex and thorough structure−activity relationship study of the CGRP C-terminal segments [Y^{27}]CGRP(27−37)-NH_2 and CGRP(27−37)-NH_2. The aim of this exercise was to identify CGRP pharmacophoric groups that are essential for receptor binding. These efforts led to a CGRP antagonist, [D^{31},P^{34},F^{35}]CGRP(27−37)-NH_2, with low nanomolar affinity (IC_{50} = 29 nM) for the $hCGRP_1$ receptor. A similar peptide containing an alanine at position 34 rather than a proline also bound to the $hCGRP_1$ receptor with reasonable affinity (IC_{50} = 159 nM). Removal of the first two residues in this latter peptide, furthermore, did not impair receptor binding. The shortest known CGRP C-terminal peptide with reasonable $hCGRP_1$ receptor affinity is thus [D^{31},A^{34},F^{35}]CGRP(29−37)-NH_2. Preliminary CD conformational investigations were carried out for [D^{31},P^{34},F^{35}]-CGRP(27−37)-NH_2, an equipotent analogue [P^{34},F^{35}]CGRP-(27−37)-NH_2, and several weaker analogues with different levels of substitution at positions 31 and 34 (*23*). Most notable was a loss of both secondary structure and receptor affinity when the phenylalanine at position 35 in [P^{34},F^{35}]-CGRP(27−37)-NH_2 was replaced with its parent peptide precursor glutamic acid.

This paper describes detailed conformational properties of five CGRP C-terminal peptide analogues as determined by NMR spectroscopy (Table 1). Two of the peptides studied are among the CGRP(27−37)-NH_2 analogues reported by Rist et al. showing good $hCGRP_1$ receptor affinity (*22*). These include [D^{31},A^{34},F^{35}]CGRP(27−37)-NH_2 and [D^{31},P^{34},F^{35}]CGRP(27−37)-NH_2. The remaining three peptides are the result of further structure−activity relationship analyses of these peptides and include [A^{34},F^{35}]CGRP(27−37)-NH_2, [A^{34},F^{35}]CGRP(28−37)-NH_2, and [D^{31},P^{34},F^{35}]-CGRP(30−37)-NH_2. The main structural difference that subdivides the peptides into two separate classes is the amino acid at position 34. Peptides in the first class contain an alanine at position 34, while those in the second class possess a proline at this position.

MATERIALS AND METHODS

Peptide Synthesis. The linear peptides were synthesized on a solid support using a Symphony multiple-peptide synthesizer and standard coupling procedures. The polymer starting material was Fmoc-Rink-amide-MBHA resin (Novabiochem) with a loading capacity of 0.6 mmol/g of resin. HATU served as the coupling reagent. The crude peptides were cleaved from the resin by a TFA/triisopropylsilane/thioanisole/H_2O mixture (94:2:2:2) and then isolated by ether precipitation. Peptides were subsequently purified to homogeneity by preparative chromatography on a Hitachi HPLC instrument equipped with a Jupiter RP-18 column (250 mm × 22 mm). The synthesized products were obtained in high yield. Homogeneity of the peptides was established by analytical HPLC in two different solvent systems on a Vydac 218TP54 or Jupiter RP-18 column with a gradient of 10 to 35 or 20 to 50% acetonitrile in 0.1% TFA (water), respec-

tively, over 25 min at 40 °C using a Hewlett-Packard 1050 HPLC system. The integration of the HPLC chromatograms recorded at 215 and 280 nm indicated a purity of at least 98%. The identity of the purified peptides was confirmed on an LCT mass spectrometer (micromass) equipped with an elecrospray source and a time-of-flight mass detector (ES-TOF) and by NMR spectroscopy.

SK-N-MC Cell Membranes. Membranes from SK-N-MC cells, a human neuroepithelioma cell line endogenously expressing the CGRP receptor, were purchased from Receptor Biology (Beltsville, MD) and kept at −80 °C until they were used.

Receptor Binding Assay. The affinity of the various CGRP analogues for the receptor was assessed through competition binding experiments using 20 pM [^{125}I]αCGRP [(3-[^{125}I]-iodohistidyl^{10})calcitonin gene-related peptide, human recombinant, IM184, Amersham Pharmacia Biotech, Little Chalfront, Buckinghamshire, England] and varying concentrations of the CGRP analogue. The membranes were diluted to give a final protein concentration of approximately 240 μg/mL. Incubation was performed at room temperature for 1 h in 96-well plates in 50 mM Tris buffer containing 5 mM $MgCl_2$, 0.1% bovine serum albumin, and 100 μM guanosine triphosphate (pH 7.4) in a final volume of 200 μL. Incubation was terminated by filtration onto glass fiber filters (Filtermat B, Wallac, Turku, Finland), pretreated with 0.3% polyethyleneimine (PEI) and rapid washing with 50 mM ice-cold Tris buffer with 5 mM $MgCl_2$ (pH 7.4) using a Skatron cell harvester (Skatron, Lier, Norway). To enhance measurement throughput, β- rather than γ-radiation was measured using a 1450 Microbeta Plus apparatus (Wallac). The level of nonspecific binding was defined as the amount of radioactivity remaining in the presence of 10 μM hαCGRP(8−37) (Bachem, Bubendorf, Switzerland).

Calculations of K_i Values. IC_{50} values were calculated using Excel Fit. The Cheng−Prusoff equation was then used to yield the K_i values.

Sample Preparation. Samples for NMR analyses were prepared by dissolving 1.0−1.4 mg of lyophilized peptide and 31 mg of SDS-d_{25} (Bio-Rad) in 500 μL of 50 mM sodium phosphate buffer [90% H_2O/10% D_2O (pH 6.8)]. The peptide and SDS final concentrations were 2.5 and 200 mM, respectively. The sample pH was consistently measured as 6.8, and samples were used without further adjustment.

Preparation of samples for FTIR measurement required adding 500 μL of SDS D_2O buffer [200 mM SDS in 50 mM phosphate buffer (100% D_2O; pH 6.8)] to 1.0−1.4 mg quantities of lyophilized peptides. All peptides readily dissolved.

NMR Spectroscopy. NMR spectra were recorded on a Bruker Avance 600 MHz spectrometer at 27 °C unless stated otherwise. Assignment of the proton chemical shifts was made using standard procedures. For each peptide, individual amino acid spin systems were first identified from a TOCSY spectrum acquired with a 50 ms mixing time. Analysis of a 100 ms NOESY spectrum completed the sequential assignments. All two-dimensional spectra were acquired in the phase-sensitive mode, using the States−TPPI method. Each two-dimensional data set typically contained 512 points in F_1 and 2K data points in F_2 with spectral widths of 6000 Hz in each dimension. Zero filling to 2K points and phase-shifted sine-squared window functions were applied along the F_1 and F_2 axes during spectral processing. Three NOESY spectra were collected for each CGRP analogue with mixing times of 50, 100, and 200 ms. Consistencies among the spectra indicated cross-peak intensities were not influenced by spin diffusion. Water suppression was achieved using the WATERGATE technique (*24*). ^{1}H chemical shifts were referenced to (3,3,3-trimethylsilyl)propionate (TSP). The vicinal $^3J_{\alpha\beta}$ coupling constants were measured from the peak-to-peak separation of well-defined multiplets in one-dimensional spectra acquired for the peptides with a digital resolution of 0.1 Hz/point.

FTIR Spectroscopy. Infrared spectra were acquired at room temperature with a PARAGON 1000 Perkin-Elmer FT-IR spectrometer interfaced with a mid-infrared detector (DTGS). Spectral data were collected at 1 cm^{-1} resolution. Assembly of the sample apparatus involved placing small aliquots of the sample (∼20 μL) between demountable CaF_2 windows separated by a 25 μm spacer. Subtraction of the background signal arising from the sample buffer was carried out automatically during each spectral acquisition. This required initial collection of a background spectrum from SDS buffer alone. Data processing was performed with the Perkin-Elmer software. Signal band narrowing was achieved using the self-deconvolution methodology when needed.

Structure Calculations. NOEs observed in the 100 ms NOESY spectra acquired for CGRP peptides [D^{31},A^{34},F^{35}]-CGRP(27−37)-NH_2 and [D^{31},P^{34},F^{35}]CGRP(27−37)-NH_2 (analogues **3** and **8**, Table 1) were classified according to their intensities as strong, medium, or weak. The intensities were then translated into distance constraints with weak, medium, and strong corresponding to 5.0, 3.5, and 2.5 Å, respectively. The lower distance bounds were set to 1.8 Å in all cases. Calculations were performed using the X-PLOR module of the InsightII software package (MSI Inc., version 98.0) and with the CHARMm force field, on a Silicon Graphics Indigo2 workstation.

For each peptide, an extended starting structure was hand-built using the Biopolymer module supplied with the Insight II software package. A set of 50 initial structures was then created by subjecting this starting structure to a distance geometry (DG) algorithm (X-PLOR/DGSA routine of InsightII) incorporating NOE-derived distance constraints, followed by constrained simulated annealing (SA). The SA component of the calculations consisted of 1000 steps of dynamics at 1000 K followed by gradual cooling to 300 K over 1000 steps. The V^{28}−P^{29} ω angle was set to 180° during the calculations since signals arising from a cis minor conformer around this peptide bond were not observed in any of the NMR spectra. H-Bonding constraints were not employed during the calculations. Pseudoatom corrections for methyl groups and methylene protons that were not stereospecifically assigned were performed automatically with the center averaging method.

The 50 starting structures were refined by several cycles of constrained simulated annealing. In this procedure, simulated annealing was performed on initial structures generated from the DGSA routine using 1000 steps at 2000 K followed by 1000 steps during which time the molecule was allowed to cool to 300 K. A time step of 0.001 ps was employed throughout the calculations. The structures were then energy minimized with 1000 steps of conjugate gradient minimization. The whole cycle was repeated 10 times.

Members of the final set of 50 structures were analyzed by the X-PLOR analysis routine, for their compatibility with the NMR data and for their conformational integrity.

RESULTS

Receptor Binding Studies of CGRP Peptides. CGRP(27−37)-NH_2 analogues shown in Table 1 were tested for their ability to bind to the $hCGRP_1$ receptor expressed in SK-N-MC cell membranes. This cell line selectively expresses the $hCGRP_1$ receptor. Binding data for two of the 10 peptides were previously reported by Rist et al. using a similar binding assay (*22*). These data are included in parentheses (Table 1) adjacent to values from this study. The $hCGRP_1$ receptor binding affinity of the potent CGRP antagonist, α-CGRP-(8−37)-NH_2, was also included in Table 1 as a standard. A review of the data in Table 1 emphasizes the advantages of a P^{34},F^{35} substitution within CGRP(27−37)-NH_2 as was previously shown by Rist et al. (*22*). Analogue **8** proved to have as high a $hCGRP_1$ receptor affinity as the CGRP antagonist CGRP(8−37)-NH_2. Replacing the proline at position 34 with an alanine was also well tolerated, although this generally led to a 5-fold decrease in receptor affinity (analogue **3**; Table 1). Incorporation of the natural amino acid N^{31} into the peptide sequence in place of an aspartic acid had a minimal effect on receptor binding in the case of $[D^{31},A^{34},F^{35}]$CGRP(27−37)-NH_2 (**3** and **4**). A similar observation has also been made for $[D^{31},P^{34},F^{35}]$CGRP(27−37)-NH_2 (**8**) [Rist et al. (*22*)].

Truncating $[D^{31},P^{34},F^{35}]$CGRP(27−37)-NH_2 (**8**) from the N-terminus by three residues (**9**) did not significantly diminish $hCGRP_1$ affinity. A dramatic loss of receptor interaction was however observed upon elimination of the fourth residue (T^{30}). Systematic removal of residues from the N-terminus of analogue **4** produced an identical trend of results (Table 1).

A particularly interesting observation was the abolishment of receptor affinity afforded by conversion of the C-terminal amide to a carboxyl in the case of $[A^{34},F^{35}]$CGRP(28−37) (analogue **2**). In a previous study, the N-terminally carboxylated form of the CGRP antagonist CGRP(8−37) [CGRP-(8−37)-OH] failed to stimulate a cyclic AMP response in osteoblast-like cells, although its CGRP receptor affinity was never assessed (*25*). Hence, $[A^{34},F^{35}]$CGRP(28−37)-OH (**2**) is the first example of a CGRP C-terminal peptide analogue rendered incapable of $hCGRP_1$ receptor binding through modification of its C-terminal cap with the attached F^{37} left intact.

Alanine Scan. An alanine scan was performed on compound $[A^{34},F^{35}]$CGRP(28−37)-NH_2 to identify important side chain determinants for $hCGRP_1$ receptor binding. The results are summarized in Table 2. There were only three cases where an alanine substitution was accompanied by a significant loss of receptor affinity. The implicated residues included T^{30}, V^{32}, and F^{37}. Alanine substitution in all other positions was well tolerated.

NMR Chemical Shift Assignments. NMR studies were carried out on five of the CGRP peptides listed in Table 1, including $[D^{31},A^{34},F^{35}]$CGRP(27−37)-NH_2 (**3**), $[A^{34},F^{35}]$-CGRP(27−37)-NH_2 (**4**), $[A^{34},F^{35}]$CGRP(28−37)-NH_2 (**5**), $[D^{31},P^{34},F^{35}]$CGRP(27−37)-NH_2 (**8**), and $[D^{31},P^{34},F^{35}]$CGRP-(30−37)-NH_2 (**9**). The ^1H NMR chemical shift assignments

Table 2: Alanine Scan of $[A^{34},F^{35}]$CGRP(28−37)-NH_2

peptide	sequence	binding ([^{125}I]CGRP) SK-N-MC mem K_i (nM)
$[\mathbf{A^{28}},A^{34},F^{35}]$CGRP(28−37)-$NH_2$	**A**PTNVGAFAF-NH_2	150 ± 59
$[\mathbf{A^{29}},A^{34},F^{35}]$CGRP(28−37)-$NH_2$	V**A**TNVGAFAF-NH_2	623 ± 45
$[\mathbf{A^{30}},A^{34},F^{35}]$CGRP(28−37)-$NH_2$	VP**A**NVGAFAF-NH_2	9800 ± 4300
$[\mathbf{A^{31}},A^{34},F^{35}]$CGRP(28−37)-$NH_2$	VPT**A**VGAFAF-NH_2	463 ± 68
$[\mathbf{A^{32}},A^{34},F^{35}]$CGRP(28−37)-$NH_2$	VPTN**A**GAFAF-NH_2	21300 ± 11000
$[\mathbf{A^{33}},A^{34},F^{35}]$CGRP(28−37)-$NH_2$	VPTNV**A**AFAF-NH_2	2030 ± 510
$[A^{34},\mathbf{A^{35}}]$CGRP(28−37)-NH_2	VPTNVGA**A**AF-NH_2	1230 ± 76
$[A^{34},F^{35},\mathbf{A^{37}}]$CGRP(28−37)-$NH_2$	VPTNVGAFA**A**-NH_2	>30000

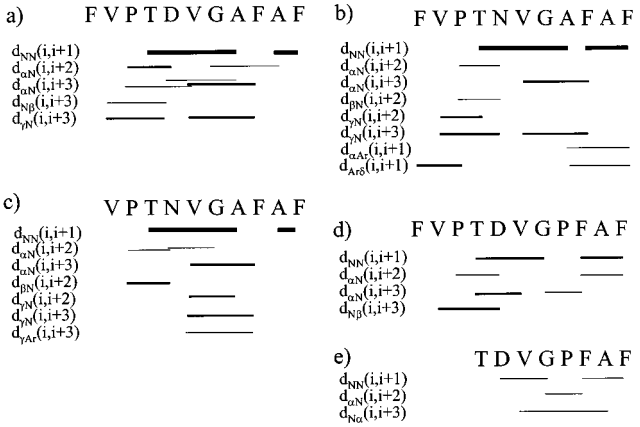

FIGURE 2: Summary of medium-range and sequential amide proton NOEs for CGRP analogues (a) **3**, (b) **4**, (c) **5**, (d) **8**, and (e) **9**. The line thickness reflects the NOE intensity, with the thinnest line corresponding to a weak signal and the thickest line representing a strong NOE intensity.

were first made using the standard procedure. A second set of NMR signals arising from a stable minor conformation was observed for the two peptides containing a proline at position 34 [$[D^{31},P^{34},F^{35}]$CGRP(27−37)-NH_2 (**8**) and $[D^{31},P^{34},F^{35}]$CGRP(30−37)-NH_2 (**9**)]. It was determined through analysis of the NMR spectra that the two stable conformers are characterized by cis and trans $G^{33}-P^{34}$ peptide bonds, respectively. In the case of $[D^{31},P^{34},F^{35}]$-CGRP(27−37)-NH_2 (**8**), the cis conformer was almost as abundant as the trans conformer as judged by the similar peak intensities measured for the two resultant sets of NMR signals. By contrast, NMR signals corresponding to the cis conformer of $[D^{31},P^{34},F^{35}]$CGRP(30−37)-NH_2 (**9**) were weaker than those arising from its trans counterpart. Removal of residues 27−29 from the N-terminus of $[D^{31},P^{34},F^{35}]$-CGRP(27−37)-NH_2, therefore, destabilizes the cis Pro^{34} conformation yet does not influence $hCGRP_1$ receptor affinity. On the basis of this result, it can be hypothesized that the bioactive conformation of peptides in the proline series contain a trans $G^{33}-P^{34}$ peptide bond. Hence, only data collected for the major trans conformers of each peptide were considered during further conformational studies.

Secondary Structure from Nuclear Overhauser Enhancements. Information about the secondary structure of the CGRP analogues was obtained through analyses of their NOESY spectra cross-peak patterns. Interresidue NOE cross-peaks were labeled as weak medium or strong according to the strength of their respective NOE signal intensities. The data are summarized in Figure 2. All peptides with the exception of $[D^{31},P^{34},F^{35}]$CGRP(30−37)-NH_2 (**9**) exhibited

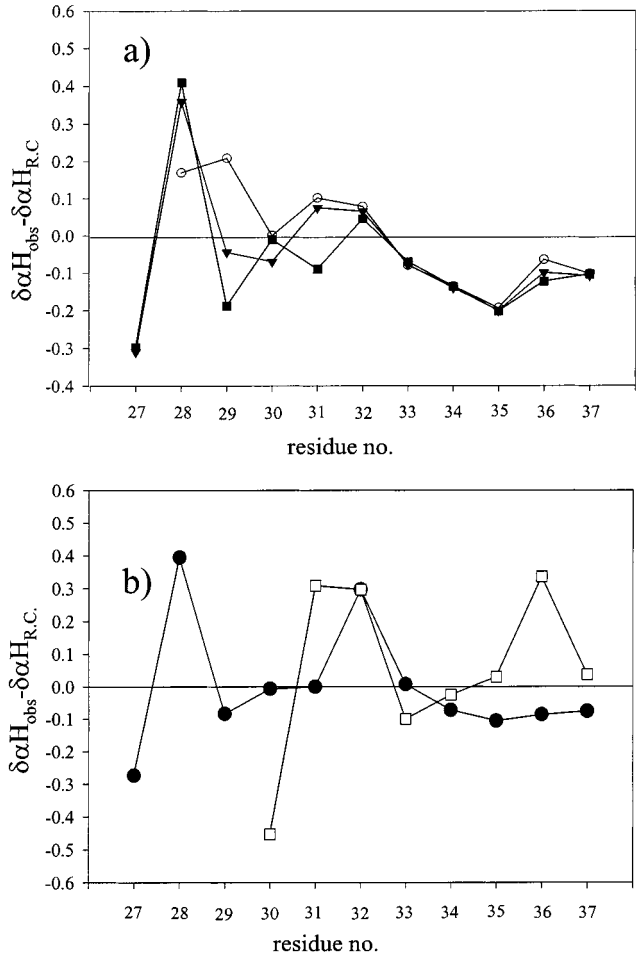

FIGURE 3: Deviation of the αH chemical shifts from random coil values ($\delta\alpha H_{obs} - \delta\alpha H_{RC}$) measured for the (a) A^{34} series [(■) **3**, (▼) **4**, and (○) **5**] and (b) P^{34} series [(●) **8** and (□) **9**].

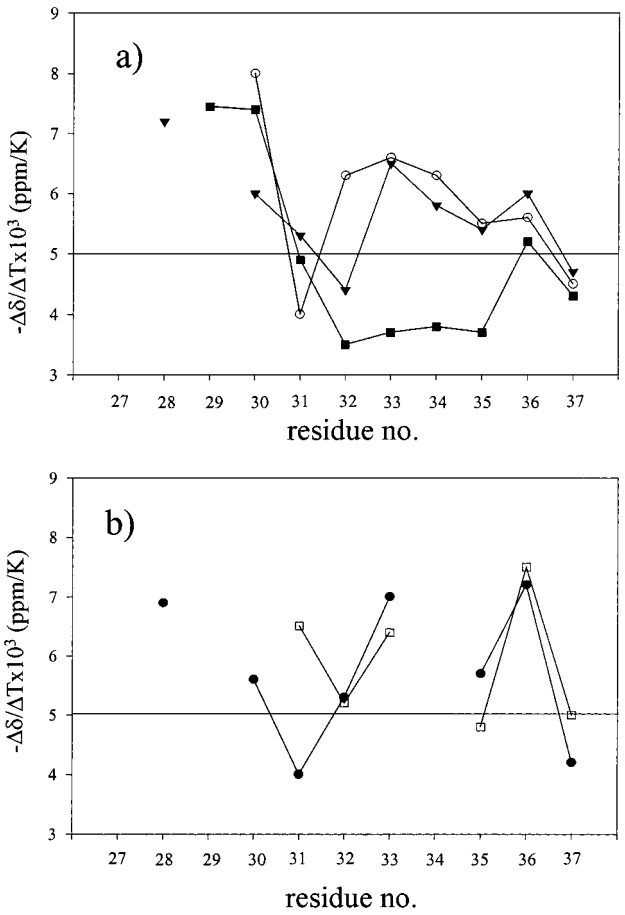

FIGURE 4: Amide proton temperature coefficients for CGRP(27−37)-NH_2 analogues in the (a) A^{34} series [(■) **3**, (▼) **4**, and (○) **5**] and (b) P^{34} series [(●) **8** and (□) **9**].

a high density of medium-range NOEs in the N-terminus between V^{28} and D^{31}/N^{31}. The most plausible explanation for this trend is the adoption of a *β*-turn structure around P^{29}.

A second noteworthy feature in Figure 2 is the large number of NOEs between V^{32} and A^{36} consistently observed for the peptides in the A^{34}-substituted series. Clearly, the C-terminus of peptides within this series also adopts some stable secondary structure. In contrast, NOEs within the C-terminus of the two peptides containing a proline at position 34 were considerably more sparse, suggesting comparatively more flexibility in this region. This greater flexibility explains the ability of peptides in the P^{34}-substituted series to readily adopt both cis and trans conformations about the $G^{33}-P^{34}$ peptide bond.

Analysis of αH Chemical Shifts. Further definition of the secondary conformational features describing the CGRP peptide analogues was realized through chemical shift analyses of their α-protons (*26*). A summary of the data is shown in Figure 3. Results for peptides in the A^{34} substitution series are graphed in Figure 3a. A high degree of αH chemical shift similarity within the region of $V^{32}-F^{37}$ is noted among the three peptides in this series. Chemical shift displacements relative to random coil values, furthermore, consistently surpassed the 0.1 ppm upfield cutoff used to distinguish a helical conformation from a random one. Thus, all three A^{34}-substituted CGRP analogues possess some degree of helical conformation from V^{32} to F^{37}. Abrupt directional changes in the αH chemical shift displacement relative to random coil values occurred at the N-terminus of both A^{34}-substituted peptides possessing an N-terminal phenylalanine. This chemical shift pattern most likely arises as a result of a *β*-turn centered on P^{29} (*26*).

Analogue [D^{31},P^{34},F^{35}]CGRP(27−37)-NH_2 (**8**) also exhibited some dramatic reversal of chemical shift displacement at the N-terminus, suggesting it may also adopt a turn around its N-terminal proline.

Temperature Dependence of Amide Proton Signals. The dependence of the amide proton chemical shifts upon temperature was used to identify intramolecular hydrogen bonding sites in each CGRP analogue. In this analysis, the extent of resonance migration as a function temperature is translated to a temperature coefficient which in turn reflects the degree of NH solvent exposure. In general, a significantly populated H-bonded form of an amide proton will yield a temperature coefficient of <5. Temperature coefficients for the two series of compounds are shown in Figure 4. Common to all peptides studied with the exception of [D^{31},P^{34},F^{35}]-CGRP(30−37)-NH_2 (**9**) was the low-temperature coefficient measured for residue 31 regardless of the nature of its side chain. This suggests that the D^{31} (or N^{31}) backbone NH is engaged in a hydrogen bond. Since the N-terminally truncated analogue [D^{31},P^{34},F^{35}]CGRP(30−37)-NH_2 (**9**) is the only peptide without this hydrogen bonding trait, one can speculate that the hydrogen bond acceptor is N-terminal to

Table 3: $^3J_{\alpha\beta}$ Coupling Constants for CGRP(27−37)-NH_2 Analogues

peptide	$^3J_{\alpha\beta}$ (Hz)			
	F^{27}	N^{31} or D^{31}	F^{35}	F^{37}
FVPTDVGAFAF-NH_2	5.5, 9.2	4.2, 9.0	7.0, 7.9	5.3, 9.2
FVPTNVGAFAF-NH_2	4.8, 8.8	5.1, 8.7	7.6, 7.6	3.9, 8.3
VPTNVGAFAF-NH_2		6.1, 7.5	7.0, 7.0	5.3, 8.8
TDVGPFAF-NH_2		4.1, 9.8	4.3, 9.2	*a*
FVPTDVGPFAF-NH_2	*a*	*a*	4.0, 9.9	*a*, 11.0

[a] Coupling constants could not be measured due to spectral overlap.

amino acid 31. A hydrogen bond of this nature could stabilize a β-turn around P^{29}.

$^3J_{\alpha\beta}$ Coupling Constants. Side chain orientations of individual residues in the studied peptides were estimated through analysis of their vicinal $^3J_{\alpha\beta}$ coupling constants. When the two measured $^3J_{\alpha\beta}$ couplings for a particular amino acid were similar and in the range of 6−8, its side chain was deemed flexible. Pairs of $^3J_{\alpha\beta}$ vicinal coupling constants weighted toward more extreme and opposing values indicated a χ_1 in the vicinity of 180° (trans) or −60° (gauche−). Cutoff values for $^3J_{\alpha\beta}(1)$ of $\leq$5.5 and $^3J_{\alpha\beta}(2)$ of $\geq$8.5 Hz for the small and large coupling constants, respectively, were employed to qualify residues into this latter category. Table 3 reports a summary of the $^3J_{\alpha\beta}$ data for CGRP peptides **3**−**5**, **8**, and **9**. According to the data in Table 3, peptides in the A^{34} series possessing an N-terminal phenylalanine (compounds **3** and **4**) contained three residues with structurally well-defined side chains. These included F^{27}, D^{31} (or N^{31}), and F^{37}. By contrast, the side chain of F^{35} is free to rotate in this series. A slight increase in the flexibility of the N^{31} side chain was noted when the N-terminal phenylalanine was removed (analogue **5**). Peptides in the P^{34} series possessed a comparatively more structurally constrained F^{35} side chain but otherwise paralleled peptides in the A^{34} series with respect to their $^3J_{\alpha\beta}$ data.

FTIR Spectroscopy. Further confirmation of the presence of a β-turn within the CGRP analogues was obtained through analyses of FTIR spectra acquired for **3**−**5**, **8**, and **9**. An amide I band appeared at 1670−1672 cm^{-1} in all cases. Previous comprehensive FTIR studies of proteins have assigned this stretching frequency to turn structures (*27*). Therefore, all five CGRP peptides investigated by both FTIR and NMR spectroscopy possess a turn conformation somewhere along the sequence. With the exception of analogue **9**, this turn is most likely centered on P^{29} based on the NMR evidence. The β-turn in analogue **9** likely resides at P^{34} since there are insufficient residues in the N-terminus to form a stable turn around P^{29}.

Molecular Modeling. CGRP analogues **3** and **8** were subjected to distance geometry calculations followed by simulated annealing. A total of 50 structures were generated for each peptide. Medium-range distance constraints derived from the NOE data as well as backbone sequential αH−NH and NH−NH NOE constraints were employed during the calculations. Distances classified as medium-range corresponded to NOEs bridging i,(i + 2) or i,(i + 3) pairs of residues. There were no long-range NOEs observed for either peptide.

In the case of [D^{31}, A^{34}, F^{35}]CGRP(27−37)-NH_2 (**3**), structures were calculated using eight medium-range and 22 sequential distance constraints. There were 26 structures in all that satisfied the entire set of NOEs. Only two of the remaining 24 conformers exhibited multiple NOE violations. The largest NOE violation did not exceed 1.0 Å, and there were no NOE-associated distances exceeding 6 Å. The most prominent feature noted within the ensemble of structures was a well-defined β-turn centered on P^{29} (rmsd = 0.73 Å; Figure 5). Backbone torsion angles between V^{28} and D^{31} possessed values characteristic of a β-turn structure in 30 of the 50 conformations that were generated. This turn was stabilized by a hydrogen bond between the D^{31} NH and the V^{28} carbonyl. A second conformational trait common to most of the generated structures and in agreement with the αH chemical shift data (Figure 3) was a helical turn at the C-terminus from V^{32} to A^{36}. Both left-handed and right-handed helical orientations were observed, although the former occurred more often and appeared in 23 of the 50 structures. Distances between pairs of the critical side chains (T^{30}, V^{32}, and F^{37}) were analyzed for all conformers possessing the C-terminal helical turn. The γ-carbon was used as a measurement point in the case of F^{37} and V^{32}, whereas the β-carbon served as the measurement starting atom for T^{30}. Interestingly, when a left-handed helical turn was present, there was little variation in the spacial arrangement of side chains for the three important residues. The T^{30}−V^{32}, F^{37}−V^{32}, and F^{37}−T^{30} inter-side chain distances were respectively 8 ± 1, 11 ± 1, and 17 ± 2 Å, respectively. The spacing between the side chains in the right-handed helical turn series was considerably more random. A superposition of eight of the structures illustrating the left-handed helical turn from V^{32} to A^{36} is shown in Figure 6. Attempts were made to superimpose sets of conformers along the entire peptide sequence. However, it was not possible to obtain converged conformations at the two ends of the peptide simultaneously. Some flexibility thus remains in the hinge point between D^{31} and V^{32}.

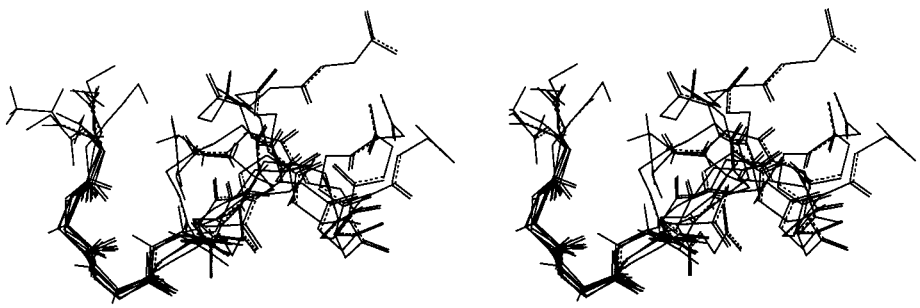

FIGURE 5: Superposition of eight of the final MD NMR-refined structures for [D^{31},A^{34},F^{35}]CGRP(27−37)-NH_2 (analogue **3**) illustrating the β-turn centered on P^{29}.

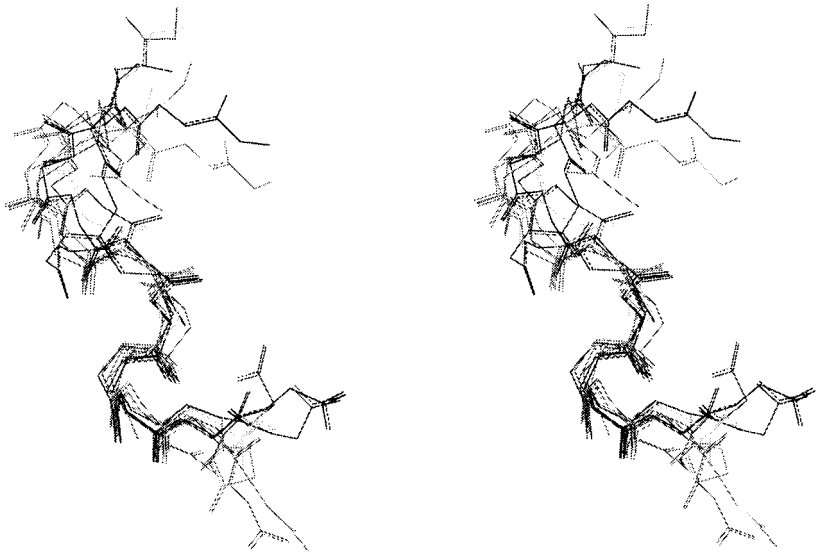

FIGURE 6: C-Terminal helix in [D^{31},A^{34},F^{35}]CGRP(27−37)-NH_2 demonstrated through a superposition of eight of the final MD NMR-refined structures calculated for analogue **3**.

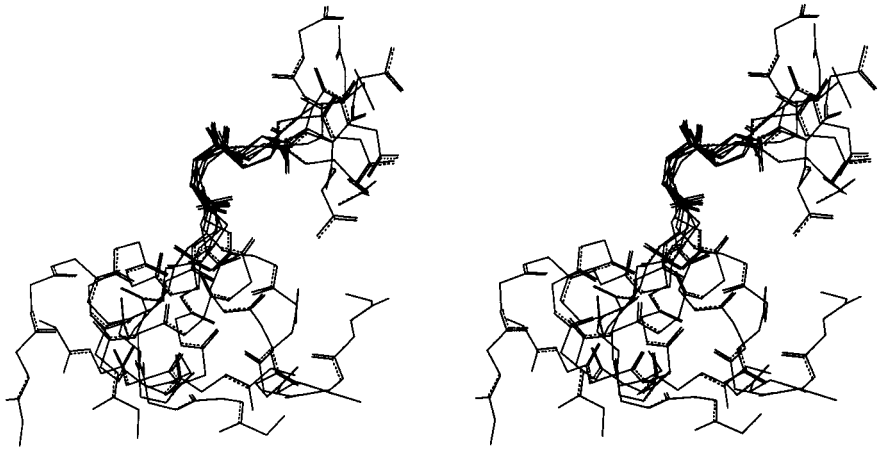

FIGURE 7: Superposition of eight of the final MD NMR-refined structures for [D^{31},P^{34},F^{35}]CGRP(27−37)-NH_2 (analogue **8**) illustrating the γ-turn centered on P^{34}.

Examination of the side chain conformational preferences for residues F^{27}, D^{31}, and F^{37} of analogue **3** revealed a couple of noteworthy points. In the case of D^{31}, a trans side chain configuration was more favorable than either gauche+ or gauche− and occurred in 28 of the 50 structures. Interestingly, this conformational feature was evident primarily when the CGRP analogue's N-terminus possessed a β-turn. A more random sampling of the three possible side chain orientations occurred for the two phenylalanines (F^{27} and F^{37}).

An ensemble of conformations was generated for the second peptide, [D^{31},P^{34},F^{35}]CGRP(27−37)-NH_2 (analogue **8**), using five medium-range and 22 sequential NOE-derived distance constraints. Only nine of the resultant 50 structures exhibited a single NOE violation. CGRP peptide **8** was viewed as being overall more disordered in its C-terminus compared to [D^{31},A^{34},F^{35}]CGRP(27−37)-NH_2 (analogue **3**). This result is not surprising considering cis and trans conformations of the G^{33}−P^{34} peptide bond in peptide **3** were equally populated. However, in the computational analysis of peptide **8**, the G^{33}−P^{34} peptide bond was restricted to be trans. In this case, 60% of the generated all-trans conformers contained a γ-turn centered on P^{34} (Figure 7). The propensity to adopt a C-terminal turn thus exists for analogue **8** as well. More agreement between the two peptides was however noted in the N-terminal region. Analogue **8** also possessed a well-defined β-turn in the V^{28}−D^{31} region (rmsd = 0.6 Å) that resulted in an exposed T^{30} side chain. This conformational feature occurred in 50% of the calculated structures. The β-turn centered on P^{29} was consistently secured by a V^{28} carbonyl to D^{31} NH hydrogen bond. A trans D^{31} side chain was found in half of the structures calculated for peptide **8** which frequently coincided with the presence of an N-terminal β-turn. A more random sampling of the side chain orientation was observed for F^{35} and F^{37} among the set of calculated conformers.

DISCUSSION

Described in this manuscript are the results of conformational studies and SAR studies carried out on two series of CGRP(27−37)-NH_2 analogues distinguished primarily by their amino acid at position 34. Although some conformational differences were noted between peptides belonging to the A^{34} series versus the P^{34} series, there were other more important elements common to both. A stable β-turn centered on P^{29} was a characteristic feature in both analogues (**3** and **8**) investigated jointly by computational methods and NMR spectroscopy. The β-turn is secured by a hydrogen bond between the carbonyl of V^{28} and the NH of D^{31}. A low amide

temperature coefficient was measured for D^{31} in both cases, thus providing further evidence for the presence of this hydrogen bond. The remaining CGRP analogues examined by NMR spectroscopy, with the exception of **9**, also exhibited a high density of medium-range NOEs at the N-terminus (Figure 2) in addition to low D^{31} (N^{31}) amide temperature coefficients (Figure 4). It is likely that they adopt a stable β-turn centered on P^{29} as well. Previous NMR investigations of the CGRP(8−37)-NH_2 antagonist in DMSO revealed a similar hydrogen bonding pattern (*19*). A slowly exchanging N^{31} amide proton was observed in this case. The ensemble of NMR refined structures reported from the same study contained 17 structures with a V^{28}−N^{31} hydrogen bond. Therefore, the CGRP(8−37)-NH_2 antagonist may also have a propensity to form a turn centered on P^{29}, although the authors claimed there were insufficient NMR data to provide a well-converged structure for this peptide in DMSO.

Additional supportive evidence for a β-turn stems from the chemical shift data. The absence of NMR signals representing a minor cis V^{28}−P^{29} solution conformation in all peptides that have been studied suggests a lack of N-terminal flexibility. Furthermore, a large positive αH chemical shift deviation from random coil values was observed for V^{28} in peptides **3**, **4**, and **8**, which was both followed by and preceded by residues exhibiting significant negative αH chemical shift displacements. This type of behavior has been linked to the occurrence of reverse-turn structures in peptides (*26*). Analogue **5** containing one fewer amino acid N-terminally did not exhibit this characteristic pattern of chemical shifts, suggesting it may be more flexible.

Compatibility between the models calculated for [D^{31},A^{34},F^{35}]CGRP(27−37)-NH_2 (**3**) and [D^{31},P^{34},F^{35}]CGRP-(27−37)-NH_2 (**8**) and the experimental $^3J_{\alpha\beta}$ coupling constant data were assessed. More extreme $^3J_{\alpha\beta}$ coupling constants were determined for the D^{31} residue in both CGRP peptides, suggesting the D^{31} side chain is somewhat restricted to adopt either a trans or gauche− configuration. These results are consistent with the modeling investigations, which produced a high proportion of conformers possessing simultaneously a trans D^{31} side chain configuration and a β-turn located at P^{29}. Thus, the D^{31} χ_1 torsion angle is likely restricted to approximately 180° due to formation of a β-turn at the peptide's N-terminus. According to the $^3J_{\alpha\beta}$ coupling constants, side chain orientational preferences were also weighted toward either trans or gauche− for residues F^{35} and F^{37} in the case of analogue **8** and for residues F^{27} and F^{37} in the case of CGRP peptide **3** (Table 3). However, there was no single associated χ_1 torsion angle that surfaced significantly more often than the other two for any of these residues during the computational studies. It is possible that one or more of the aromatic side chains are restricted by a hydrophobic interaction with the SDS micelles. Alternatively, there may have been insufficient NOEs recorded from the NOESY spectra for their conformational definition due to spectral overlap of the aromatic ring protons. Nevertheless, the consistent side chain separations involving T^{30}, V^{32}, and F^{37} in conformers of analogue **3** containing a left-handed helical turn were not influenced by the apparent F^{37} flexibility observed during modeling studies.

According to the NOE-derived molecular models generated for **3** and **8**, the N-terminal β-turn results in the T^{30} side chain being completely exposed to the outside surroundings of the molecule. Substitution of the threonine with an alanine in CGRP C-terminal peptides [Y^{27}]CGRP(27−37)-NH_2 (*22*) and [A^{34},F^{35}]CGRP(28−37)-NH_2 (analogue **5**) resulted in a complete loss of receptor affinity (Table 2). The side chain of this residue is thus critical for the peptide's biological activity. Threonine likely interacts directly with the $hCGRP_1$ receptor rather than acting as a conformational stabilizing functionality since its importance is apparently independent of the CGRP analogue amino acid sequence. Other important evidence for this hypothesis is obtained from the peptide structure−activity studies. N-Terminal truncation in both the A^{34} and P^{34} series of CGRP analogues was well tolerated up to T^{30}. However, once the threonine was removed, receptor affinity dropped dramatically. The shortest CGRP analogue (peptide **9**) studied by NMR spectroscopy with good receptor affinity did not have any ordered conformation. It is therefore expected that the N-terminal threonine residue of this peptide is also exposed to the surroundings and is thus easily available for a receptor interaction.

Two additional residues were identified as being important for biological activity based on results from the alanine scan (Table 2). They are V^{32} and F^{37}. Loss of $hCGRP_1$ receptor affinity has also been reported for [Y^{27}]CGRP(27−37)-NH_2 following an alanine substitution at either of these residue positions as well as at T^{30} (*22*).The C-terminal F^{37} is particularly critical for activity. Any attempts to remove this residue from CGRP or its analogues have resulted in a large decrease in CGRP1 receptor affinity (*20*). Changing the amino acid chirality at position 37 was also accompanied by a reduction in the level of receptor binding (*22*). Interestingly, replacement of the C-terminal amide in [A^{34},F^{35}]-CGRP(28−37)-NH_2 with a carboxyl group abolished CGRP1 receptor affinity (analogue **2**; Table 1). Therefore, it appears that the uncharged amide functionality attached to CGRP's C-terminus is a critical player in mediating a CGRP receptor interaction. Whether the F^{37}-NH_2 pharmacophoric group plays a structural role or interacts with the receptor directly is not known. However, previous conformational investigations of CGRP and its CGRP(1−36)-NH_2 analogue did not reveal any distinguishable conformational differences between the two peptides (*28*). Thus, the latter hypothesis involving a direct receptor interaction is more plausible.

A key finding from the molecular modeling investigations of [D^{31},A^{34},F^{35}]CGRP(27−37)-NH_2 (analogue **3**) was a consistent spatial arrangement of the three critical residues whenever a left-handed helical turn occupied its C-terminus. According to the series of generated structures for this peptide, the latter feature represents a significant proportion of the peptide's conformational ensemble. It may thus be hypothesized that the N-terminal β-turn and C-terminal helical turn in analogue **3** together promote a correct geometrical arrangement of residues T^{30}, V^{32}, and F^{37} for receptor binding. A similar trend was not observed for the other computationally analyzed active CGRP analogue [D^{31},P^{34},F^{35}](27−37)-NH_2 despite finding a stable β-turn at the N-terminus and a γ-turn structure at the C-terminal end of the peptide. Hence, [D^{31},P^{34},F^{35}](27−37)-NH_2 may be too flexible to adopt a more tightly folded conformation in the aqueous micelle solution. Conformationally relevant NOEs were fewer in number, and cis−trans isomerization around P^{34} was evident in its associated NMR spectra. It is possible

that further stabilization of a turn centered on P^{34} may follow from an initial interaction of the peptide with the CGRP1 receptor which, in turn, could promote a preferred arrangement of the T^{30}, V^{32}, and F^{37} residues for receptor activation.

CONCLUSIONS

Models for CGRP C-terminal peptides [D^{31},A^{34},F^{35}]CGRP-(27−37)-NH_2 and [D^{31},P^{34},F^{35}]CGRP(27−37)-NH_2 were computed using the NMR parameters as constraints. A β-turn centered on the N-terminal proline was a notable feature common to both peptides. This feature persisted in all other CGRP analogues containing at least one amino acid N-terminal to P^{29} and, furthermore, resulted in exposure of the critical threonine to the surrounding environment. An additional stable C-terminal helical turn found in [D^{31},A^{34},F^{35}]-CGRP(27−37)-NH_2 resulted in its critical pharmacophoric groups exhibiting a fixed orientation with respect to one another. The N- and C-terminal turn structures found in CGRP(27−37)-NH_2 analogues may thus play an important role in positioning key residues (T^{30}, V^{32}, and F^{37}) required for a successful $hCGRP_1$ interaction.

REFERENCES

1. Amara, S. G., Jonas, V., Rosenfeld, M. G., Ong, E. S., and Evans, R. M. (1982) *Nature 298*, 240−244.
2. Amara, S. G., Arriza, J. L., Leff, S. E., Swanson, L. W., Evans, R. M., and Rosenfeld, M. G. (1985) *Science 229*, 1094−1097.
3. Steenbergh, P. H., Hoppener, J. W., Zandberg, J., Lips, C. J., and Jansz, H. S. (1985) *FEBS Lett. 183*, 403−407.
4. Moskowitz, M. A. (1984) *Ann. Neurol. 16*, 157−168.
5. Goadsby, P. J., Zagami, A. S., and Lambert, G. A. (1991) *Headache 31*, 365−371.
6. Goadsby, P. J., Edvinsson, L., and Ekman, R. (1990) *Ann. Neurol. 28*, 183−187.
7. Gallai, V., Sarchielli, P., Floridi, A., Franceschini, M., Codini, M., Glioti, G., Trequattrini, A., and Palumbo, R. (1995) *Cephalalgia 15*, 384−390.
8. Kapas, S., and Clark, A. J. (1995) *Biochem. Biophys. Res. Commun. 217*, 832−838.
9. Quirion, R., Van Rossum, D., Dumont, Y., St-Pierre, S., and Fournier, A. (1992*) Ann. N.Y. Acad. Sci. 657*, 88−105.
10. Dennis, T., Fournier, A., St-Pierre, S., and Quirion, R. (1989) *J. Pharmacol. Exp. Ther. 251*, 718−725.
11. Maggi, C. A., Rovero, P., Giuliani, S., Evangelista, S., Regoli, D., and Meli, A. (1990) *Eur. J. Pharmacol. 179*, 217−219.
12. Saha, S., Waugh, D. J., Zhao, P., Abel, P. W., and Smith, D. D. (1998) *J. Pept. Res. 52*, 112−120.
13. Rovero, P., Giuliani, S., and Maggi, C. A. (1992) *Peptides 13*, 1025−1027.
14. Maton, P. N., Pradhan, T., Zhou, Z. C., Gardner, J. D., and Jensen, R. T. (1990) *Peptides 11*, 485−489.
15. Chakder, S., and Rattan, S. (1990) *J. Pharmacol. Exp. Ther. 253*, 200−206.
16. Manning, M. C. (1989) *Biochem. Biophys. Res. Commun. 160*, 388−392.
17. Hubbard, J. A., Martin, S. R., Chaplin, L. C., Bose, C., Kelly, S. M., and Price, N. C. (1991) *Biochem. J. 275*, 785−788.
18. Breeze, A. L., Harvey, T. S., Bazzo, R., and Campbell, I. D. (1991) *Biochemistry 30*, 575−582.
19. Boulanger, Y., Khiat, A., Chen, Y., Senecal, L., Tu, Y., St.-Pierre, S., and Fournier, A. (1995) *Pept. Res. 8*, 206−213.
20. Boulanger, Y., Khiat, A., Larocque, A., Fournier, A., and St. Pierre, S. (1996) *Int. J. Pept. Protein Res. 47*, 477−483.
21. Saldanha, J., and Mahadevan, D. (1991) *Protein Eng. 4*, 539−544.
22. Rist, B., Entzeroth, M., and Beck-Sickinger, A. G. (1998) *J. Med. Chem. 41*, 117−123.
23. Rist, B., Lacroix, J. S., Entzeroth, M., Doods, H. N., and Beck-Sickinger, A. G. (1999) *Regul. Pept. 79*, 153−158.
24. Piotto, M., Saudek, V., and Sklenar, V. (1992) *J. Biomol. NMR 2*, 661−665.
25. Thiebaud, D., Akatsu, T., Yamashita, T., Suda, T., Noda, T., Martin, R. E., Fletcher, A. E., and Martin, T. J. (1991) *J. Bone Miner. Res. 6*, 1137−1142.
26. Wishart, D. S., Sykes, B. D., and Richards, F. M. (1992) *Biochemistry 31*, 1647−1651.
27. Jackson, M., and Mantsch, H. H. (1995) *Crit. Rev. Biochem. Mol. Biol. 30*, 95−120.
28. O'Connell, J. P., Kelly, S. M., Raleigh, D. P., Hubbard, J. A. M., Price, N. C., Dobson, C. M., and Smith, B. J. (1993) *Biochem. J. 291*, 205−210.

BI0102860